Electronic Supplementary Material (ESI) for Journal of Materials Chemistry A.
This journal is © The Royal Society of Chemistry 2021

Electronic Supplementary Information

Single atom catalysts for boosting electrocatalytic and photoelectrocatalytic performances

Shijun Tong,[a] Baihe Fu,[a] Liyong Gan*[b] and Zhonghai Zhang*[a]

[a] Shanghai Key Laboratory of Green Chemistry and Chemical Processes, School of Chemistry and Molecular Engineering, East China Normal University, Shanghai 200241, China.
E-mail: zhzhang@chem.ecnu.edu.cn
[b] Institute for Structure and Function and Department of Physics, Chongqing University, Chongqing, 400030, China.
E-mail: ganly@cqu.edu.cn

Table of Contents:

I. Additional Figures and Tables

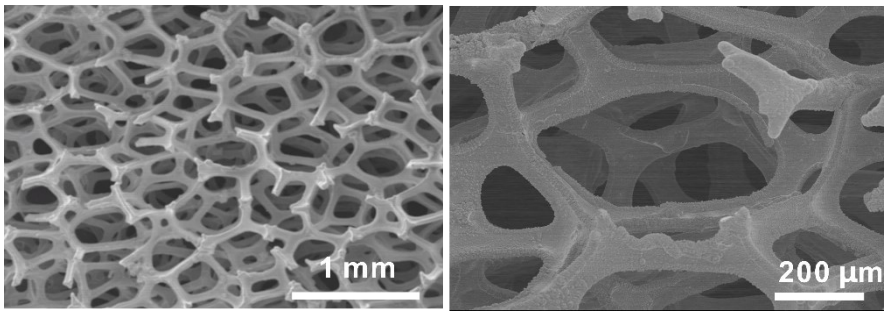

Fig. S1 SEM images of NF.

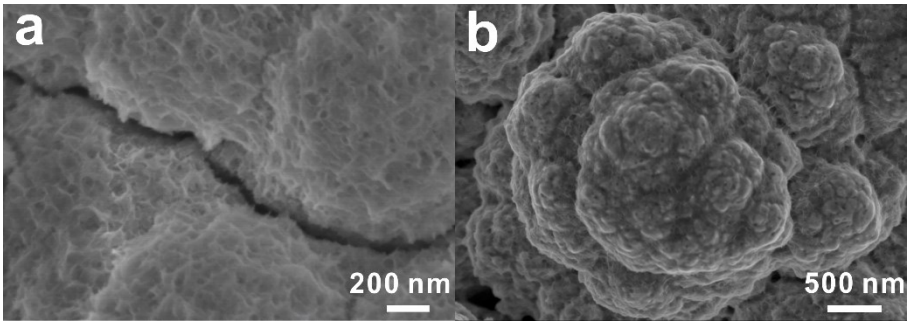

Fig. S2 SEM images of (a) Ni/NF and (b) N-Ni/NF.

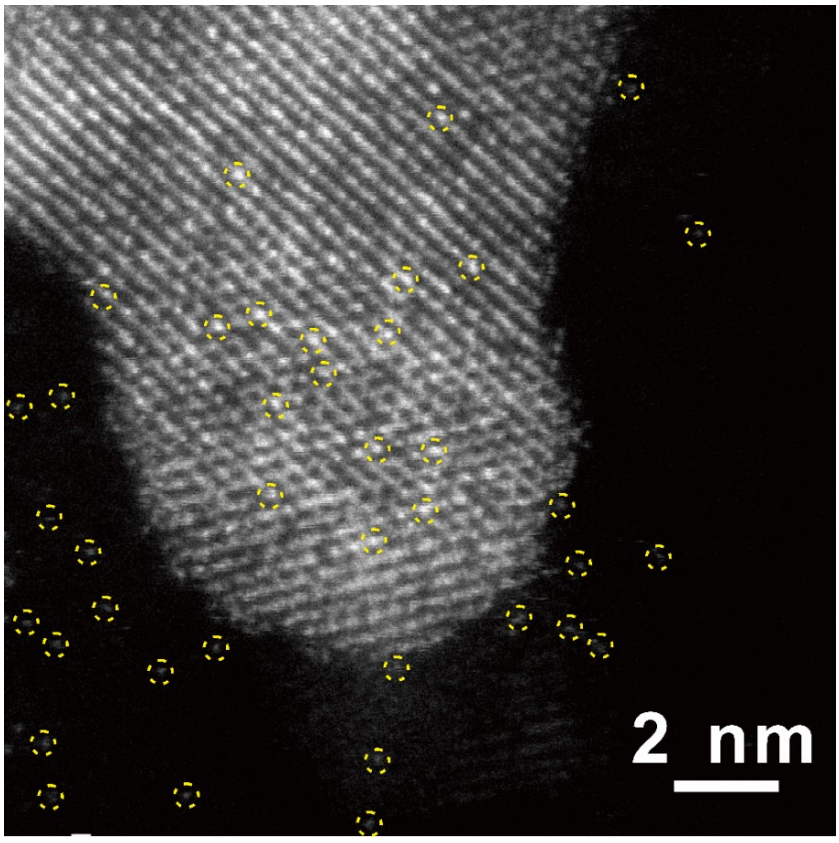

Fig. S3 Enlarged AC HAADF-STEM image of Pt single atoms in Fig. 1c.

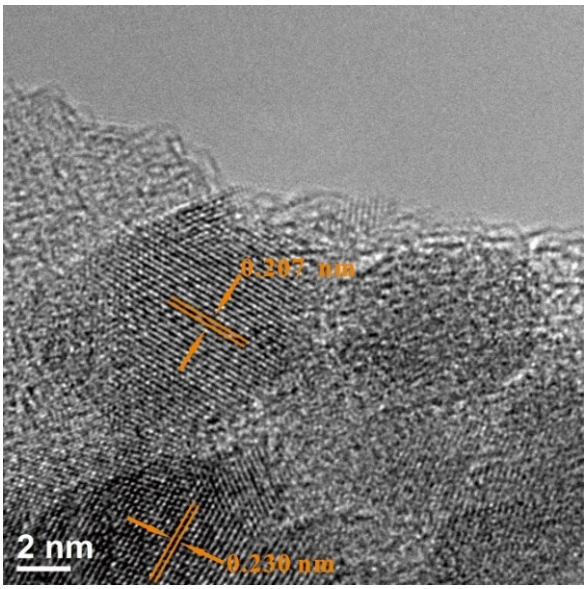

Fig. S4 HRTEM image of Pt NPs/N-Ni/NF.

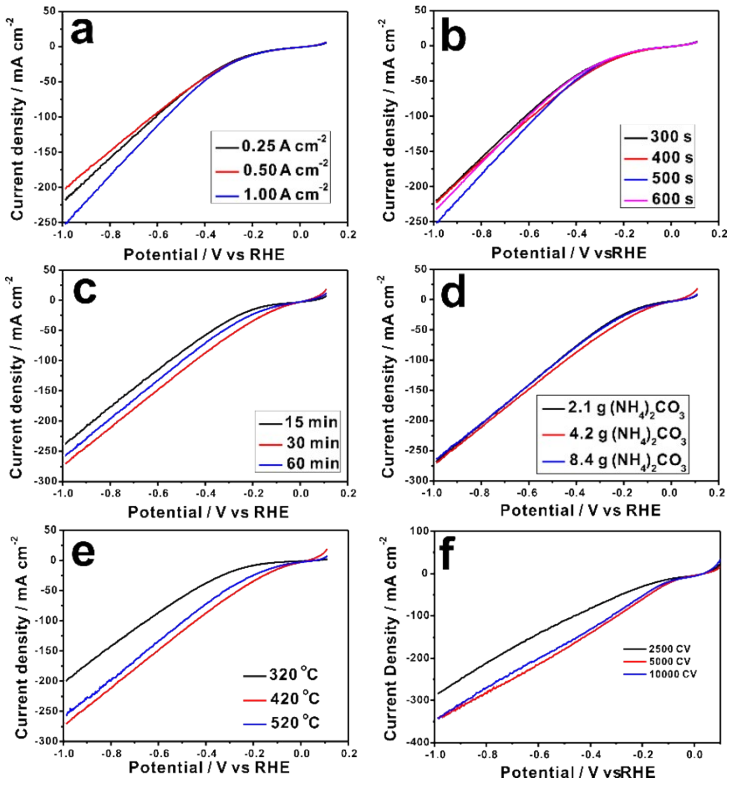

Fig. S5 Electrochemical HER performance of Ni/NF deposited at (a) different current density and (b) different time; N-Ni/NF annealed at (c) different time with (d) different amounts of $(NH_4)_2CO_3$, and (e) different temperatures; (f) Pt_1/N-Ni/NF deposited after different potential cycles.

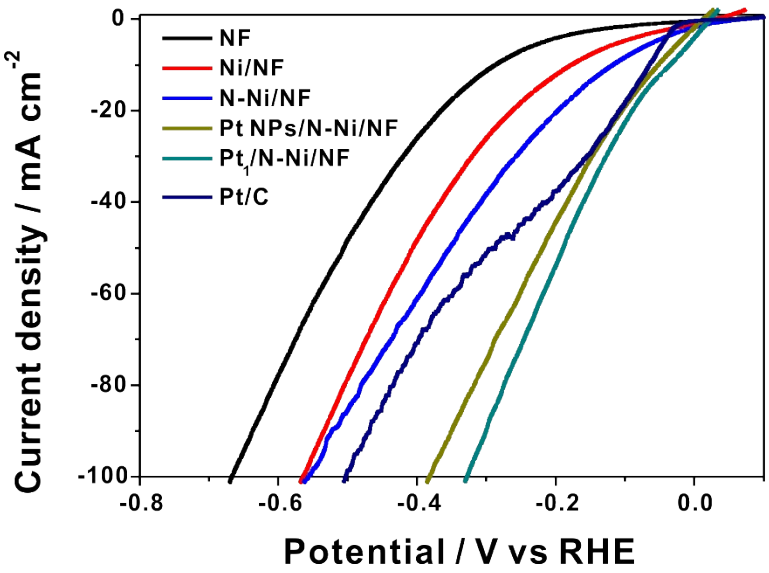

Fig. S6 LSV curves for HER of NF, Ni/NF, N-Ni/NF, Pt NPs/N-Ni/NF, Pt_1/N-Ni/NF, and Pt/C in 1 M PBS with high current density.

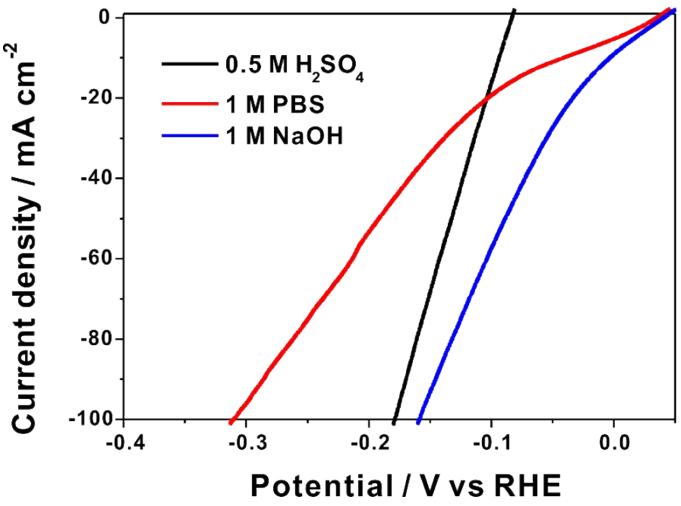

Fig. S7 LSV curves for HER of Pt_1/N-Ni/NF in acidic, neutral, and alkaline electrolytes.

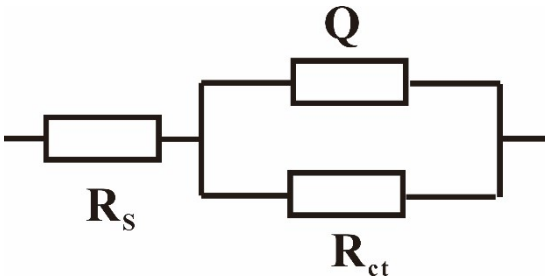

Fig. S8 Fitted equivalent circuits of EIS data.

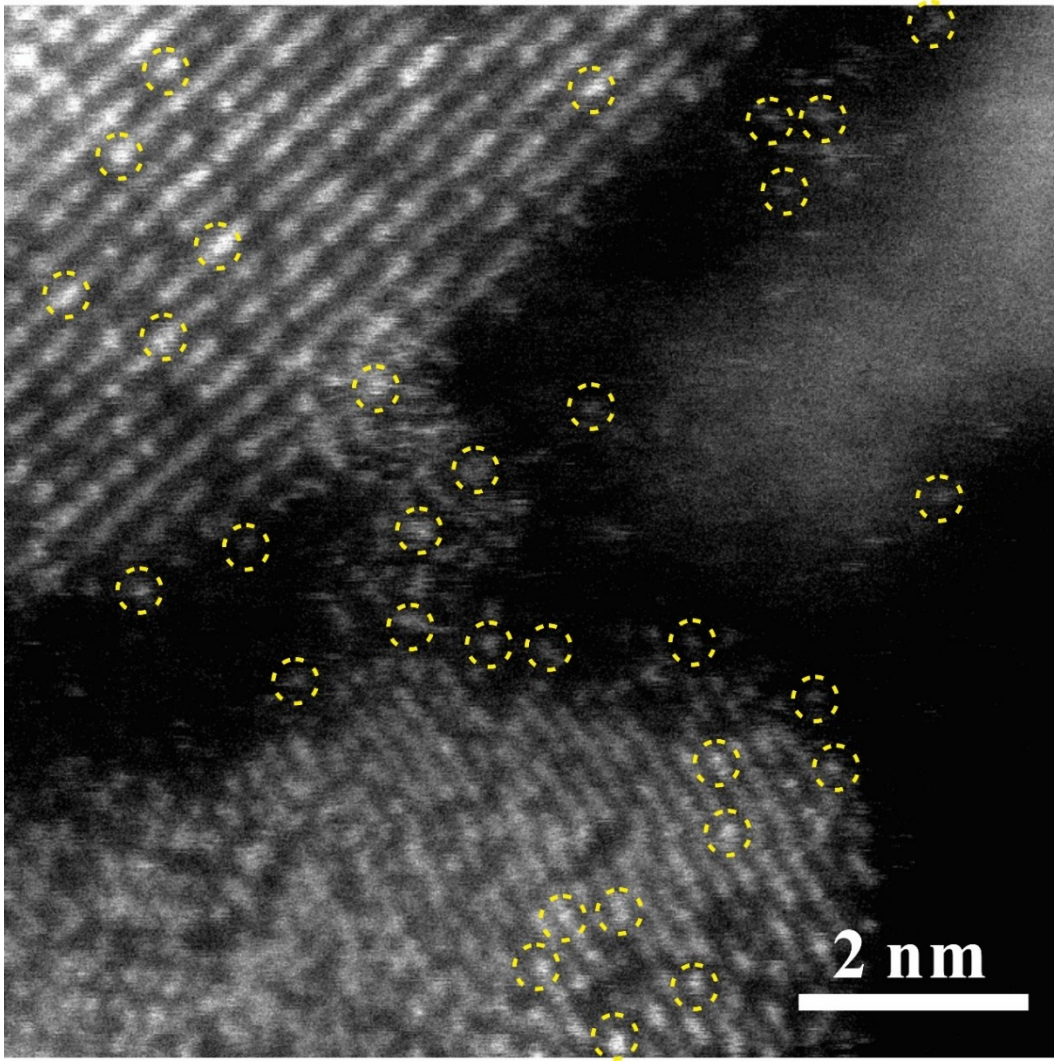

Fig. S9 AC HAADF-STEM image of Pt_1/N-Ni/NF over 24h stability test.

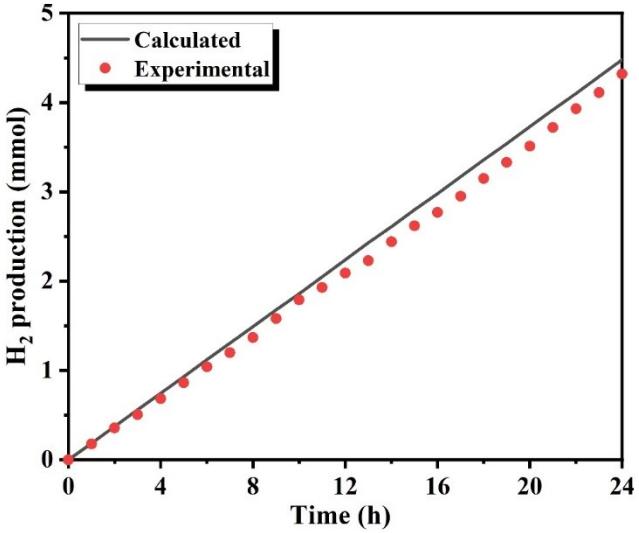

Fig. S10 The theoretical and experimental values of H_2 for HER during 24 stability test of Pt_1/N-Ni/NF at a constant current density of 10 mA cm^{-2}.

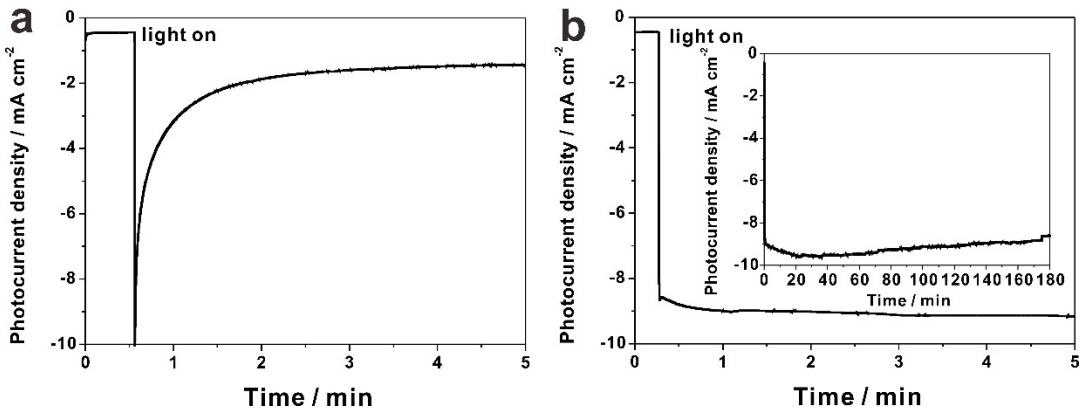

Fig. S11 PEC stability measurements on (a) pristine Cu_2O and on (b) Pt_1/N-Ni/Cu_2O at potential of 0 V vs RHE.

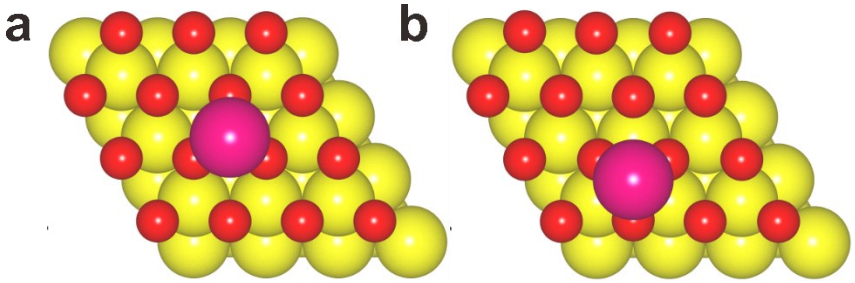

Fig. S12 Top view of modeled Pt_1/N-Ni SAC with the Pt atom located above the (a) first and (b) second Ni layer. The yellow, red, and pink balls represent Ni, N and Pt atoms, respectively.

Table R1. Equivalent circuit model for EIS plots fitting.

Sample	NF	Ni/NF	N-Ni/NF	Pt_1/N-Ni/NF
R_s(ohm/cm^2)	6.258	5.745	6.041	6.183
Q	0.000159	0.0001787	0.01507	0.1796
R_{ct}(ohm/cm^2)	817.2	71.16	34.06	3.313

R_s: solution resistance; Q: capacitance of the double layer; R_{ct}: charge transfer resistance.

Table S2. EC HER performance of this work and other reported electrocatalysts in neutral media.

Electrocatalyst	electrolyte	[a]η_{10} (mV)	Stability	References
$Ni_{0.33}Co_{0.67}S_2$	1.0 M PBS	72	20 h at 70 mV ([b]η)	S1
CoO/$CoSe_2$	0.5 M PBS	337	9 h at ~ 337 mV or 2000 cycles	S2
SiO_2/PPy NTs-CFs	1.0 M PBS	183	30 h at 200 mV(η)	S3
Co-HNP/CC	1.0 M PBS	85	20 h at -150 mA/cm^2	S4
FeO_x/FeP	1.0 M PBS	96	60 h at multi-	S5

			potential(η)	
$NiCoP_x$	1.0 M PBS	63	30 h at -100 mV(η)	S6
N-Ni	1.0 M PBS	64	18 h at -20 mA/cm^2	S7
CrO_x/Cu-Ni/Cu foam	1.0 M PBS	48	24 h at 100 mV(η)	S8
$Ni_{0.89}Co_{0.11}Se_2$ MNSN/NF	1.0 M PBS	82	40 h at 200 mV(η)	S9
$Ni_{0.1}Co_{0.9}P$	1.0 M PBS	125	20 h at -30 mA/cm^2	S10
$CoMoS_4$ NTA/CC	1.0 M PBS	104	32 h at 142 mV(η)	S11
Mn-Co-P/Ti	1.0 M PBS	86	10 h at 96 mV(η) or 1000 cycles	S12
FeP/Ti	1.0 M PBS	102	16 h at -10 mA/cm^2	S13
$CoW(OH)_x$	1.0 M PBS	73.6	70 h at -20 mA/cm^2	S14
Ni-Mo-S/C	0.5 M PBS	200	30000 s	S15
GC|Cu-Cu_xO-Pt-1	2.0 M PBS	35	100 h at 55 mV(η)	S16
CoP/CC	1.0 M PBS	106	1000 cycles	S17
MoP_2/MoP	1.0 M PBS	75	4000 cycles	S18
Ni/NiMoN array	0.5 M Na_2SO4 +0.5 M PBS	37	24 h at 37 mV(η)	S19
Mn-Ni-S/NF	1.0 M PBS	84	24 h at 180 mV(η) or 5000 cycles	S20
v-NiFe LDH	1.0 M PBS	87	1000 cycles	S21
Fe@N-CNT/IF	1.0 M PBS	130	10 h at multi-potential(η)	S22
$Zn_{0.075}$,S-$Co_{0.925}P$ NRCs/CP	1.0 M PBS	67	20 h at -10 mA/cm^2 or 1000 cycles	S23
N-CoP/CC	1.0 M PBS	74	30 h at -10 mA/cm^2 or 1000 cycles	S24
PEI@NiP_2-CC	1.0 M PBS	100	20 h at -10 mA/cm^2	S25
Ru@SC-CDs	1.0 M PBS	66	5000 cycles	S26
$FePSe_3$/NC	1.0 M PBS	140.1	24 h at -10 mA/cm^2	S27
Ru-RuO_2/CNT	1.0 M PBS	48	10 h at 40 mV(η) or 1500 cycles	S28
RuS_x/S-GO	1.0 M PBS	46	12 h for -50 mA/cm^2	S29
W-CoP NAs/CC	1.0 M PBS	102	36 h at 102 mV(η) or 2000 cycles	S30
NFP/C	1.0 M PBS	117	12 h at -10 mA/cm^2	S31
$Co_{0.6}Fe_{0.4}P$/CNT	1.0 M PBS	105	24 h for -10 mA/cm^2 or 5000 ADT cycles	S32
$(Fe_{0.048}Ni_{0.952})_2P$	1.0 M PBS	90	20 h for -100 mA/cm^2 or 1000 cycles	S33
CoP/Co-MOF	1.0 M PBS	49	60000 s at -20 mA/cm^2 or 2000	S34

			cycles	
VN@Ni_3N-Ni-6/CC	1.0 M PBS	85	30 h at 85 mV(η) or 3000 cycles	S35
np-$Co_9S_4P_4$	1.0 M PBS	87	20 h for -10 mA/cm^2	S36
N-Co2P/CC	1.0 M PBS	42	120000 s for -10 mA/cm^2 or 3000 cycles	S37
Karst NF	1.0 M PBS	110	10 h at 210 mV(η)	S38
CoS_x-(0.2-0.02)-12	1.0 M PBS	182	20 h at -10 mA/cm^2	S39
Mn-NiO-Ni/Ni-F	1.0 M PBS	80	55 h at 80 mV(η)	S40
$Ni(S_{0.5}Se_{0.5})_2$	1.0 M PBS	124	20 h at 125 mV(η) or 2000 cycles	S41
$Cu_{0.08}Co_{0.92}P$ NAs/CP	1.0 M PBS	81	20 h at -10 mA/cm^2 or 3000 cycles	S42
$Ni_{0.85}Se$@NC	1.0 M PBS	183	10 h at 183 mV(η) or 2000 cycles	S43
RhCoB	1.0 M PBS	113	10 h at -10 mA/cm^2 or 2000 cycles	S44
3D RuCu NCs	0.01 M PBS	73	12 h for ~ -10 mA/cm^2 or 3000 cycles	S45
Fe-(NiS_2/MoS_2)/CNT	1.0 M PBS	127	8 h at -10 mA/cm^2	S46
Pt_1/N-Ni/NF	1.0 M PBS	33	24 h at -10 mA/cm^2	This work

[a] η_{10} = overpotential required to reach current density of -10 mA/cm^2. [b] η = overpotential.

Table S3. PEC HER performance of this work and other reported Cu_2O based photocathodes.

Photoelectrode	Photocurrent density (mA cm^{-2}) at 0 V vs RHE	References
NiMo/Ga_2O_3/Cu_2O NWs	10	S47
RuOx/TiO_2/AZO/Cu_2O NWs	10	S48
Pt/TiO_2/AZO/Cu_2O	7.6	S49
TiO_2/Ga_2O_3/Cu_2O/CuSCN	6.4	S50
RuO_2/TiO_2/AZO/Cu_2O	5.16	S51
NiS/Cu_2O/Al	5.0	S52
$Ti_3C_2T_x$/Cu_2O	4.45	S53
Ni/CuO/Cu_2O	4.3	S54
Pt/TiO_2/AZO/Ga_2O_3/Cu_2O	4.0	S55
Cu_2MoS_4/NiO/Cu_2O	1.25	S56
Pt_1/N-Ni/NF	11.9	This work

II. Additional References

(S1) Peng, Z.; Jia, D.; Al-Enizi, A. M.; Elzatahry, A. A.; Zheng, G. From Water Oxidation to Reduction: Homologous Ni–Co Based Nanowires as Complementary Water Splitting Electrocatalysts. *Adv. Energy Mater*. **2015**, *5*, 1402031.

(S2) Li, K.; Zhang, J.; Wu, R.; Yu, Y.; Zhang, B. Anchoring CoO Domains on $CoSe_2$ Nanobelts as Bifunctional Electrocatalysts for Overall Water Splitting in Neutral Media. *Adv. Sci*. **2016**, *3*, 1500426.

(S3) Feng, J. X.; Han, X.; Ye, S. H.; Ouyang, G.; Tong, Y. X.; Li, G. R. Silica–Polypyrrole Hybrids as High-Performance Metal-Free Electrocatalysts for the Hydrogen Evolution Reaction in Neutral Media. *Angew. Chem. Int. Ed*. **2017**, *56*, 8120-8124.

(S4) Liu, B.; Zhang, L.; Xiong, W.; Ma, M. Cobalt-Nanocrystal-Assembled Hollow Nanoparticles for Electrocatalytic Hydrogen Generation from Neutral-pH Water. *Angew. Chem. Int. Ed.* **2016**, *55*, 6725-6729.

(S5) Huang, J.; Su, Y.; Zhang, Y.; Wu, W.; Wu, C.; Sun, Y.; Lu, R.; Zou, G.; Li, Y.; Xiong, J. FeO_x/FeP hybrid nanorods neutral hydrogen evolution electrocatalysis: insight into interface. *J. Mater. Chem. A* **2018**, *6*, 9467-9472.

(S6) Zhang, R.; Wang, X.; Yu, S.; Wen, T.; Zhu, X.; Yang, F.; Sun, X.; Wang, X.; Hu, W. Ternary $NiCo_2P_x$ Nanowires as pH-Universal Electrocatalysts for Highly Efficient Hydrogen Evolution Reaction. *Adv. Mater*. **2017**, *29*, 1605502.

(S7) You, B.; Liu, X.; Hu, G.; Gul, S.; Yano, J.; Jiang, D.; Sun, Y. Universal Surface Engineering of Transition Metals for Superior Electrocatalytic Hydrogen Evolution in Neutral Water. *J. Am. Chem. Soc.* **2017**, *139*, 12283-12290.

(S8) Dinh, C. T.; Jain, A.; García de Arquer, F. P.; Luna, P. D.; Li, J.; Wang, N.; Zheng, X.; Cai, J.; Gregory, B. Z.; Voznyy, O.; Zhang, B.; Liu, M.; Sinton, D.; Crumlin, E. J.; Sargent. E. H. Multi-site electrocatalysts for hydrogen evolution in neutral media by destabilization of water molecules. *Nat Energy* **2019**, *4*, 107-114.

(S9) Liu, B.; Zhao, Y. F.; Peng, H. Q.; Zhang, Z. Y.; Sit, C. K.; Yuen, M. F.; Zhang, T. R.; Lee, C. S.; Zhang. W. J. Nickel–Cobalt Diselenide 3D Mesoporous Nanosheet Networks Supported on Ni Foam: An All-pH Highly Efficient Integrated Electrocatalyst for Hydrogen Evolution. *Adv. Mater.* **2017**, *29*, 1606521.

(S10) Wu, R.; Xiao, B.; Gao, Q.; Zheng, Y. R.; Zheng, X. S.; Zhu, J. F.; Gao, M. R.; Yu, S. H. A Janus Nickel Cobalt Phosphide Catalyst for High-Efficiency Neutral-pH Water Splitting. *Angew. Chem. Int. Ed*. **2018**, *130*, 15671-15675.

(S11) Wang, W.; Ren, X.; Hao, S.; Liu, Z.; Xie, F.; Yao, Y.; Asiri, A. M.; Chen, L.; Sun. X. Self-Templating Construction of Hollow Amorphous $CoMoS_4$ Nanotube Array towards Efficient Hydrogen Evolution Electrocatalysis at Neutral pH. *Chem. Eur. J*. **2017**, *23*, 12718-12723.

(S12) Liu, T.; Ma, X.; Liu, D.; Hao, S.; Du, G.; Ma, Y.; Asiri, A. M.; Sun, X.; Chen, L. Mn Doping of CoP Nanosheets Array: An Efficient Electrocatalyst for Hydrogen Evolution Reaction with Enhanced Activity at All pH Values. *ACS catal.* **2017**, *7*, 98-102.

(S13) Callejas, J. F.; McEnaney, J. M.; Read, C. G.; Crompton, J. C.; Biacchi, A. J.; Popczun, E. J.; Gordon, T. R.; Lewis, N. S.; Schaak, R. E. Electrocatalytic and Photocatalytic Hydrogen Production from Acidic and Neutral-pH Aqueous Solutions Using Iron Phosphide Nanoparticles. *ACS Nano* **2014**, *8*, 11101-11107.

(S14) Zhang, L.; Liu, P. F.; Li, Y. H.; Wang, C. W.; Zu, M. Y.; Fu, H. Q.; Yang, X. H.; Yang, H. G. Accelerating Neutral Hydrogen Evolution with Tungsten Modulated Amorphous Metal Hydroxides. *ACS Catal*. **2018**, *8*, 5200-5205.

(S15) Miao, J.; Xiao, F. X.; Yang, H. B.; Khoo, S. Y.; Chen, J.; Fan, Z.; Hsu, Y. Y.; Chen, H. M.; Zhang, H.; Liu, B. Hierarchical Ni-Mo-S nanosheets on carbon fiber cloth: A flexible electrode for efficient hydrogen generation in neutral electrolyte. *Sci. Adv.* **2015**, *1*, e1500259.

(S16) Zhang, P.; Wang, M.; Chen, H.; Liang, Y.; Sun, J.; Sun, L. A Cu-Based Nanoparticulate Film as Super-Active and Robust Catalyst Surpasses Pt for Electrochemical H_2 Production from Neutral and Weak Acidic Aqueous Solutions. *Adv. Energy Mater*. **2016**, *6*, 1502319.

(S17) Tian, J.; Liu, Q.; Asiri, A. M.; Sun, X. Self-Supported Nanoporous Cobalt Phosphide Nanowire Arrays: An Efficient 3D Hydrogen-Evolving Cathode over the Wide Range of pH 0−14. *J. Am. Chem. Soc*. **2014**, *136*, 7587-7590.

(S18) Xie, X.; Song, M.; Wang, L.; Engelhard, M. H.; Luo, L.; Miller, A.; Zhang, Y.; Du, L.; Pan, H.; Nie, Z.; Chu, Y.; Estevez, L.; Wei, Z.; Liu, H.; Wang, C.; Li, D.; Shao, Y. Electrocatalytic Hydrogen Evolution in Neutral pH Solutions: Dual-Phase Synergy. *ACS Catal*. **2019**, *9*, 8712-8718.

(S19) Shang, L.; Zhao, Y.; Kong, X. Y.; Shi, R.; Waterhouse, G. I. N.; Wen, L.; Zhang, T. Underwater superaerophobic Ni nanoparticle-decorated nickel–molybdenum nitride nanowire arrays for hydrogen evolution in neutral media. *Nano Energy* **2020**, *78*, 105375.

(S20) Zeng, L.; Liu, Z.; Sun, K.; Chen, Y.; Zhao, J.; Chen, Y.; Pan, Y.; Lu, Y.; Liu, Y.; Liu, C. Multiple modulations of pyrite nickel sulfides via metal heteroatom doping engineering for boosting alkaline and neutral hydrogen evolution. *J. Mater. Chem. A* **2019**, *7*, 25628-25640.

(S21) Yuan, Z.; Bak, S. M.; Li, P.; Jia, Y.; Zheng, L.; Zhou, Y.; Bai, L.; Hu, E.; Yang, X. Q.; Cai, Z.; Sun, Y.; Sun, X. Activating Layered Double Hydroxide with Multivacancies by Memory Effect for Energy-Efficient Hydrogen Production at Neutral pH. *ACS Energy Lett*. **2019**, *4*, 1412-1418.

(S22) Yu, J.; Li, G.; Liu, H.; Zeng, L.; Zhao, L.; Jia, J.; Zhang, M.; Zhou, W.; Liu, H.; Hu, Y. Electrochemical Flocculation Integrated Hydrogen Evolution Reaction of Fe@N-Doped Carbon Nanotubes on Iron Foam for Ultralow Voltage Electrolysis in Neutral Media. *Adv. Sci.* **2019**, *6*, 1901458.

(S23) Yan, L.; Zhang, B.; Zhu, J.; Liu, Z.; Zhang, H.; Li, Y. Callistemon-like Zn and S codoped CoP nanorod clusters as highly efficient electrocatalysts for neutral-pH overall water splitting. *J. Mater. Chem. A* **2019**, *7*, 22453-22462.

(S24) Men, Y.; Li, P.; Yang, F.; Cheng, G.; Chen, S.; Luo, W. Nitrogen-doped CoP as robust electrocatalyst for high-efficiency pH universal hydrogen evolution reaction. *Appl. Catal. B: Environ*. **2019**, *253*, 21-27.

(S25) Ding, Y.; Miao, B. Q.; Jiang, Y. C.; Yao, H. C.; Li, X. F.; Chen, Y. Polyethylenimine-modified nickel phosphide nanosheets: interfacial protons boost the hydrogen evolution reaction. *J. Mater. Chem. A* **2019**, *7*, 13770-13776.

(S26) Liu, Y.; Yang, Y.; Peng, Z.; Liu, Z.; Chen, Z.; Shang, L.; Lu, S.; Zhang, T. Self-crosslinking carbon dots loaded ruthenium dots as an efficient and super-stable hydrogen production electrocatalyst at all pH values. *Nano Energy* **2019**, *65*, 104023.

(S27) Yu, J.; Li, W. J.; Zhang, H.; Zhou, F.; Li, R.; Xu, C. Y.; Zhou, L.; Zhong, H.; Wang, J. Metallic $FePSe_3$ nanoparticles anchored on N-doped carbon framework for All-pH hydrogen evolution reaction. *Nano Energy* **2019**, *57*, 222-229.

(S28) Zhang, M.; Chen, J.; Li, H.; Cai, P.; Li, Y.; Wen, Z. Ru-RuO_2/CNT hybrids as high-activity pH-universal electrocatalysts for water splitting within 0.73 V in an asymmetric-electrolyte electrolyzer. *Nano Energy* **2019**, *61*, 576-583.

(S29) Li, P.; Duan, X.; Wang, S.; Zheng, L.; Li, Y.; Duan, H.; Kuang, Y.; Sun, X. Amorphous Ruthenium-Sulfide with Isolated Catalytic Sites for Pt-Like Electrocatalytic Hydrogen Production Over Whole pH Range. *Small* **2019**, *15*, 1904043.

(S30) Wang, X.; Chen, Y.; Yu, B.; Wang, Z.; Wang, H.; Sun, B.; Li, W.; Yang, D.; Zhang, W. Hierarchically Porous W-Doped CoP Nanoflake Arrays as Highly Efficient and Stable Electrocatalyst for pH-Universal Hydrogen Evolution. *Small* **2019**, *15*, 1902613.

(S31) Lu, X. F.; Yu, L.; Lou, X. W. D. Highly crystalline Ni-doped FeP/carbon hollow nanorods as all-pH efficient and durable hydrogen evolving electrocatalysts. *Sci. Adv*. **2019**, *5*, eaav6009.

(S32) Zhang, X.; Zhang, X.; Xu, H.; Wu, Z.; Wang, H.; Liang, Y. Iron-Doped Cobalt Monophosphide Nanosheet/Carbon Nanotube Hybrids as Active and Stable Electrocatalysts for Water Splitting. *Adv. Funct. Mater*. **2017**, *27*, 1606635.

(S33) Zhang, W.; Zou, Y.; Liu, H.; Chen, S.; Wang, X.; Zhang, H.; She, X.; Yang, D. Single-crystalline $(Fe_xNi_{1-x})_2P$ nanosheets with dominant $\{011^{-}1^{-}\}$ facets: Efficient electrocatalysts for hydrogen evolution reaction at all pH values. *Nano Energy* **2019**, *56*, 813-822.

(S34) Liu, T.; Li, P.; Yao, N.; Cheng, G.; Chen, S.; Luo, W.; Yin, Y. CoP-Doped MOF-Based Electrocatalyst for pH-Universal Hydrogen Evolution Reaction. *Angew. Chem. Int. Ed.* **2019**, *131*, 4727-4732.

(S35) Dong, X.; Yan, H.; Jiao, Y.; Guo, D.; Wu, A.; Yang, G.; Shi, X.; Tian, C.; Fu, H. 3D hierarchical V–Ni-based nitride heterostructure as a highly efficient pH-universal electrocatalyst for the hydrogen evolution reaction. *J. Mater. Chem. A* **2019**, *7*, 15823-15830.

(S36) Tan, Y.; Luo, M.; Liu, P.; Cheng, C.; Han, J.; Watanabe, K.; Chen, M. Three-Dimensional Nanoporous $Co_9S_4P_4$ Pentlandite as a Bifunctional Electrocatalyst for Overall Neutral Water Splitting. *ACS Appl. Mater. Interfaces* **2019**, *11*, 3880-3888.

(S37) Men, Y.; Li, P.; Zhou, J.; Cheng, G.; Chen, S.; Luo, W. Tailoring the Electronic Structure of Co_2P by N Doping for Boosting Hydrogen Evolution Reaction at All pH Values. *ACS Catal*. **2019**, *9*, 3744-3752.

(S38) Gao, X.; Chen, Y.; Sun, T.; Huang, J.; Zhang, W.; Wang, Q.; Cao, R. Karst landform-featured monolithic electrode for water electrolysis in neutral media. *Energy Environ. Sci*. **2020**, *13*, 174-182.

(S39) He, W.; Ifraemov, R.; Raslin, A.; Hod, I. Room-Temperature Electrochemical Conversion of Metal–Organic Frameworks into Porous Amorphous Metal Sulfides with Tailored Composition and Hydrogen Evolution Activity. *Adv. Funct. Mater*. **2018**, *28*, 1707244.

(S40) Lu, X.; Pan, J.; Lovell, E.; Tan, T. H.; Ng, Y. H.; Amal, R. A sea-change: manganese doped nickel/nickel oxide electrocatalysts for hydrogen generation from seawater. *Energy Environ. Sci*. **2018**, *11*, 1898-1910.

(S41) Zeng, L.; Sun, K.; Chen, Y.; Liu, Z.; Chen, Y.; Pan, Y.; Zhao, R.; Liu, Y.; Liu, C. Neutral-pH overall water splitting catalyzed efficiently by a hollow and porous structured ternary nickel sulfoselenide electrocatalyst. *J. Mater. Chem. A* **2019**, *7*, 16793-16802.

(S42) Yan, L.; Zhang, B.; Zhu, J.; Li, Y.; Tsiakaras, P.; Shen, P. K. Electronic modulation of cobalt phosphide nanosheet arrays via copper doping for highly efficient neutral-pH overall water splitting. *Appl. Catal. B: Environ*. **2020**, *265*, 118555.

(S43) Huang, Z.; Xu, B.; Li, Z.; Ren, J.; Mei, H.; Liu, Z.; Xie, D.; Zhang, H.; Dai, F.; Wang, R.; Sun, D. Accurately Regulating the Electronic Structure of Ni_xSe_y@NC Core–Shell Nanohybrids through Controllable Selenization of a Ni-MOF for pH-Universal Hydrogen Evolution Reaction. *Small* **2020**, *16*, 2004231.

(S44) Deng, K.; Ren, T.; Xu, Y.; Liu, S.; Dai, Z.; Wang, Z.; Li, X.; Wang, L.; Wang, H. Transition metal M (M = Co, Ni, and Fe) and boron co-modulation in Rh-based aerogels for highly efficient and pH-universal hydrogen evolution electrocatalysis. *J. Mater. Chem. A* **2020**, *8*, 5595-5600.

(S45) Cao, D.; Wang, J.; Xu, H.; Cheng, D. Growth of Highly Active Amorphous RuCu Nanosheets on Cu Nanotubes for the Hydrogen Evolution Reaction in Wide pH Values. *Small* **2020**, *16*, 2000924.

(S46) Li, C.; Liu, M.; Ding, H.; He, L.; Wang, E.; Wang, B.; Fan, S.; Liu, K. A lightly Fe-doped (NiS_2/MoS_2)/carbon nanotube hybrid electrocatalyst film with laser-drilled micropores for stabilized overall water splitting and pH-universal hydrogen evolution reaction. *J. Mater. Chem. A* **2020**, *8*, 17527-17536.

(S47) Pan, L.; Kim, J. H.; Mayer, M. T.; Son, M. K.; Ummadisingu, A.; Lee, J. S.; Hagfeldt, A.; Luo, J.; Grätzel, M. Boosting the performance of Cu_2O photocathodes for unassisted solar water splitting devices. *Nat. Catal.* **2018**, *1*, 412-420.

(S48) Luo, J.; Steier, L.; Son, M. K.; Schreier, M.; Mayer, M. T.; Grätzel, M. Cu_2O Nanowire Photocathodes for Efficient and Durable Solar Water Splitting. *Nano. Lett.* **2016**, *16*, 1848-1857.

(S49) Paracchino, A.; Laporte, V.; Sivula, K.; Grätzel, M.; Thimsen, E. Highly active oxide photocathode for photoelectrochemical water reduction. *Nat. Mater*. **2011**, *10*, 456-461.

(S50) Pan, L.; Liu, Y.; Yao, L.; Ren, D.; Sivula, K.; Grätzel, M.; Hagfeldt, A. Cu_2O photocathodes with band-tail states assisted hole transport for standalone solar water splitting. *Nat. Commun*. **2020**, *11*, 318.

(S51) Chen, D.; Liu, Z.; Guo, Z.; Yan, W.; Ruan, M. Decorating Cu_2O photocathode with noble-metal-free Al and NiS cocatalysts for efficient photoelectrochemical water splitting by light harvesting management and charge separation design. *Chem. Eng. J*. **2020**, *381*, 122655.

(S52) Tilley, S. D.; Schreier, M.; Azevedo, J.; Stefik, M.; Graetzel, M. Ruthenium Oxide Hydrogen Evolution Catalysis on Composite Cuprous Oxide Water-Splitting Photocathodes. *Adv. Funct. Mater.* **2014**, *24*, 303-311.

(S53) Fu, X.; Chang, H.; Shang, Z.; Liu, P.; Liu, J.; Luo, H. Three-dimensional Cu_2O nanorods modified by hydrogen treated $Ti_3C_2T_X$ MXene with enriched oxygen vacancies as a photocathode and a tandem cell for unassisted solar water splitting. *Chem. Eng. J.* **2020**, *381*, 122001.

(S54) Dubale, A. A.; Pan, C. J.; Tamirat, A. G.; Chen, H. M.; Su, W. N.; Chen, C. H.; Rick, J.; Ayele, D. W.; Aragaw, B. A.; Lee, J. F.; Yang, Y. W.; Hwang, B. J. Heterostructured Cu_2O/CuO decorated with nickel as a highly efficient photocathode for photoelectrochemical water reduction. *J. Mater. Chem. A* **2015**, *3*, 12482-12499.

(S55) Wang, Y. C.; Qin, C.; Lou, Z. R.; Lu, Y. F.; Zhu, L. P. Cu_2O photocathodes for unassisted solar water-splitting devices enabled by noblemetal cocatalysts simultaneously as hydrogen evolution catalysts and protection layers. *Nanotechnology* **2019**, *30*, 495407.

(S56) Yang, C.; Tran, P. D.; Boix, P. P.; Bassi, P. S.; Yantara, N.; Wong, L. H.; Barber, J. Engineering a Cu_2O/NiO/Cu_2MoS_4 hybrid photocathode for H_2 generation in water. *Nanoscale* **2014**, *6*, 6506-6510.